GRAPHSPA: SELF-SUPERVISED GRAPH SPARSIFICATION FOR ROBUST GENERALIZATION

Anonymous authors
Paper under double-blind review

ABSTRACT

Graph sparsification has emerged as a promising approach to improve efficiency and remove redundant or noisy edges in large-scale graphs. However, existing methods often rely on task-specific labels, limiting their applicability in label-scarce scenarios, and they rarely address the residual noise that persists after sparsification. In this work, we present GRAPHSPA, a self-supervised graph sparsification framework that learns to construct compact yet informative subgraphs without requiring labels, while explicitly mitigating the effect of residual noise. GRAPHSPA formulates sparsification with a target edge budget as a constrained optimization problem, modeling each edge as a differentiable Bernoulli random variable and employing the mutual information between sampled subgraphs and the original graph as a loss function to learn individual edge importance. To progressively impose sparsity with stability, GRAPHSPA adopts an augmented Lagrangian scheme with convergence guarantees. In addition, the encoder is trained in a flatness-aware manner using Sharpness-Aware Minimization (SAM), which reduces sensitivity to residual noise and improves generalization. Extensive experiments on benchmark datasets demonstrate that GRAPHSPA consistently outperforms baselines across different sparsity ratios, preserves cluster structures in t-SNE visualizations, and remains robust even when noisy edges are injected after sparsification. These results highlight GRAPHSPA as a principled and reliable framework for graph sparsification without labels and under residual noise.

1 INTRODUCTION

Graph Neural Networks (GNNs) have achieved remarkable success in a wide range of graph learning tasks, including node classification (Kipf & Welling, 2016), link prediction (Zhang & Chen, 2018), recommender systems (Ying et al., 2018), and social network modeling (Qiu & et al., 2018). These advances demonstrate the strong potential of GNNs for analyzing complex relational data, yet scaling them to large real-world graphs remains challenging. As graph size increases, computational and memory costs grow rapidly, and real-world graphs often contain redundant or spurious edges (Li et al., 2024; Satuluri & Parthasarathy, 2011) that propagate misleading signals and degrade representation quality. Graph sparsification has emerged as a promising approach to mitigate these issues by removing redundant or noisy edges, thereby reducing overhead and yielding cleaner structural representations (Batson et al., 2013; Zheng et al., 2020). However, supervised sparsification methods rely on task-specific labels (Chen et al., 2021; Li et al., 2019), limiting their applicability in label-free scenarios such as recommender systems or social networks (Sobolevsky & Belyi, 2022; Guo et al., 2024). Meanwhile, unsupervised heuristic methods based on structural indicators such as degree or PageRank have also been explored (Batagelj & Zaversnik, 2003; Page et al., 1999). Yet these methods depend only on shallow cues and merely attempt to remove unnecessary edges, without explicitly addressing the residual noise that inevitably remains after sparsification.

Alongside reliance on labels, residual noise from sparsification poses another fundamental challenge. Since sparsification simplifies the graph structure, the diversity of propagation paths is reduced, making models more vulnerable to noisy edges (Dong & Kluger, 2023). With fewer effective signals, over-parameterized GNNs tend to overfit and become more sensitive to residual noise (Zhou et al., 2018). This issue is particularly acute in domains such as social networks, where relationships themselves act as supervision signals. Spurious edges introduced by fake accounts or ephemeral connections distort the learning process and undermine downstream tasks such as community de-

tection or link prediction (Wang et al., 2018). Addressing this challenge requires new sparsification methods that can effectively mitigate residual noise while operating without labels.

In this paper, we propose GRAPHSPA, a self-supervised graph sparsification framework designed to address both the reliance on labels and the vulnerability to residual noise. To overcome label dependence, GRAPHSPA explores diverse subgraph combinations and learns individual edge importance by comparing their mutual information with the original graph, enabling the discovery of meaningful sparsified structures without labels. To further mitigate the residual noise that inevitably remains after sparsification, GRAPHSPA jointly optimizes the encoder during sparsification by leveraging Sharpness-Aware Minimization (SAM) (Foret et al., 2021). This encourages convergence toward flat minima, reduces sensitivity to noise, and ultimately enhances generalization.

GRAPHSPA models each edge as a Bernoulli random variable and samples subgraphs according to its probability. By relaxing the discrete edge selection into continuous probabilities, the process becomes differentiable, which enables gradient propagation during training. The mutual information between the sampled subgraphs and the original graph is employed as a loss function to learn individual edge importance scores. In the early stage of training, the framework encourages broad exploration of diverse structural variants, and later progressively shifts toward concentrating on meaningful structures. To enforce the target edge budget while preserving structural information, GRAPHSPA adopts an Augmented Lagrangian scheme (Boyd et al., 2011b). Unlike one-shot sparsification, sparsity is imposed progressively with theoretical convergence guarantees, ensuring training stability. Moreover, to mitigate the effect of residual noise, the encoder is jointly optimized during sparsification by leveraging Sharpness-Aware Minimization (SAM). This guides optimization toward flat minima, reduces sensitivity to noisy edges, and improves generalization performance.

We validate the effectiveness of GRAPHSPA through extensive experiments on benchmark datasets including Cora, Citeseer, and Pubmed. Across different edge ratios, GRAPHSPA consistently outperforms existing baselines, showing better accuracy while preserving structural information. Visualization studies further confirm that GRAPHSPA maintains the cluster structure of the original graph in t-SNE embeddings, and robustness evaluations demonstrate that the framework sustains strong performance even when noisy edges are injected after sparsification. These results highlight GRAPHSPA as a reliable and generalizable framework for graph sparsification without labels.

Our main contributions are summarized as follows:

- We propose GRAPHSPA, a self-supervised graph sparsification framework that removes the reliance on labels while explicitly addressing the persistent influence of residual noise.
- We propose a unified framework that combines Bernoulli edge sampling with mutual information guided importance learning, progressive sparsification under an augmented Lagrangian formulation, and flatness aware optimization using SAM.
- We conduct extensive experiments on multiple benchmarks, demonstrating that GRAPHSPA consistently outperforms baselines across edge ratios, preserves structural integrity, and achieves strong generalization under noisy conditions.

2 RELATED WORKS

Graph Self-Supervised Learning (Graph SSL) has emerged as a powerful paradigm in graph neural network (GNN) research, attracting significant attention from both academia and industry. In graph SSL, the model is trained through well-designed auxiliary tasks, where supervisory signals are automatically generated from the data without requiring manual labels (Li et al., 2022; Liu et al., 2021). Among various approaches, contrastive learning has proven to be one of the most successful strategies for graph data (Velickovic et al., 2019; Xu et al., 2021; Zeng & Xie, 2021). Its key idea is to maximize the similarity between representations of two different augmented views of the same graph, typically by maximizing their mutual information (van den Oord et al., 2018). Such methods have achieved state-of-the-art performance in diverse graph-based downstream tasks, but research that combines graph SSL with graph sparsification remains relatively limited.

Graph Sparsification aims to construct a sparser graph by removing a subset of edges from the original graph. This reduces storage cost, accelerates GNN training and inference, and alleviates the impact of redundant or noisy edges. However, many existing sparsification methods rely heavily

on sufficient label information, which is often scarce in real-world scenarios such as recommender systems or social networks (Yang et al., 2016; Hu et al., 2020). In the absence of labels, they are largely restricted to heuristic strategies such as random or degree-based removal. A representative example is DropEdge (Rong et al., 2020), which randomly removes edges at each training epoch to improve generalization. Beyond random removal, heuristic sparsification methods based on structural indicators have also been explored, such as degree-based sparsification (Batagelj & Zaversnik, 2003), which removes edges connected to nodes with low degree or limited contribution to graph connectivity, and centrality-based sparsification (Girvan & Newman, 2002; Chen et al., 2021), which removes structurally less important edges according to centrality measures such as PageRank (Page et al., 1999). While these approaches are simple and computationally efficient, sparsification inherently simplifies the graph structure. As a result, informative edges may be inadvertently discarded or spurious ones retained, and the simplified structure becomes more vulnerable to residual noise, ultimately leading to degraded robustness and generalization performance (Xu et al., 2019; Zheng et al., 2020; Luo et al., 2021; Wu et al., 2023).

3 PRELIMINARIES

To ground our method, we first formalize the problem of graph sparsification and review the principle of flatness-aware optimization. These preliminaries establish the foundation for GRAPHSPA, which integrates self-supervised sparsification with flatness-aware training to address residual noise.

3.1 PROBLEM SETUP

We begin by representing an undirected input graph $G = (V, E)$, where V is the set of N vertices and E is the set of edges. The graph structure is described by the adjacency matrix $A \in \mathbb{R}^{N\times N}$, where $A[i, j] = 1$ if $(i, j) \in E$ and 0 otherwise. Each vertex $v \in V$ is associated with a feature vector $\mathbf{x}_v \in \mathbb{R}^F$, and the feature matrix is denoted as $X \in \mathbb{R}^{N\times F}$.

Given (A, X), GNN f_θ learns node representations by iteratively aggregating information from neighbors across layers. At the l-th layer, the representation of node v is updated as:

$$h_v^{(l+1)} = \psi\Big(h_v^{(l)},\, \phi\{h_u^{(l)} \mid u \in N_v\}\Big), \tag{1}$$

where ϕ denotes an aggregation function over neighbors, ψ combines the previous representation of v with the aggregated messages, and $h_v^{(0)} = \mathbf{x}_v$ is the initial representation.

The goal of graph sparsification is to learn a function

$$\mathcal{P} : G \to G_s, \tag{2}$$

where $G_s \subseteq G$ is a sparsified subgraph that preserves as much informative structure of G as possible. Formally, $G_s = (V, E_s)$ is defined by an adjacency matrix $A_s \in \{0, 1\}^{|E|}$, where $A_s[i, j] = 1$ if the edge $(i, j) \in E_s$ is kept and 0 otherwise. An edge retention ratio $r \in (0, 1)$ controls the proportion of edges retained, and G_s keeps $r\%$ of the original edges. In the self-supervised setting, no label information such as node labels is available. Instead, the sparsification mechanism has to identify and retain informative edges without supervision.

3.2 SHARPNESS-AWARE MINIMIZATION

Sharpness-Aware Minimization (SAM) aims to find loss minima that are not only high-performing but also insensitive to parameter perturbations, thereby improving generalization and robustness (Foret et al., 2021). Formally, SAM solves the following min–max optimization problem:

$$\min_{\theta} \max_{\|\epsilon\|\le\rho} \mathcal{L}(\theta + \epsilon), \tag{3}$$

where $\mathcal{L}(\theta)$ is the training loss for parameters θ, and ϵ denotes parameter perturbations within an ℓ_p ball of radius ρ, which determines the maximum perturbation size. The inner maximization seeks the worst-case performance under perturbations, while the outer minimization finds parameters robust

to such perturbations. To efficiently approximate the inner maximization, SAM uses a first-order Taylor expansion. The perturbation that maximally increases the loss is estimated as:

$$\hat{\epsilon} = \rho \cdot \frac{\nabla_\theta \mathcal{L}(\theta)}{\|\nabla_\theta \mathcal{L}(\theta)\|_2} \approx \arg\max_{\|\epsilon\|_p \leq \rho} \mathcal{L}(\theta + \epsilon), \tag{4}$$

At training step t, SAM is implemented via the following iterative process:

$$\epsilon_t = \nabla_\theta \mathcal{L}(\theta_t), \quad \hat{\epsilon}_t = \rho \cdot \frac{\epsilon_t}{\|\epsilon_t\|_2}, \quad \omega_t = \nabla_\theta \mathcal{L}(\theta_t + \hat{\epsilon}_t), \quad \theta_{t+1} = \theta_t - \eta \cdot \omega_t, \tag{5}$$

where ϵ_t is the perturbation gradient, $\hat{\epsilon}_t$ is the normalized perturbation within the ρ-ball, ω_t is the updating gradient evaluated at the perturbed parameters, and η is the learning rate. By updating parameters using gradients computed at perturbed weights, SAM explicitly encourages convergence to flat minima, where the loss landscape varies smoothly under small perturbations, thereby improving generalization and robustness across diverse domains (Foret et al., 2021; Baek et al., 2024).

4 GRAPHSPA

In this section, we introduce GRAPHSPA, a self-supervised graph sparsification framework that explicitly addresses residual noise while preserving the structural information of the original graph. GRAPHSPA formulates sparsification with a target edge budget as a constrained optimization problem. Instead of relying on labels, each edge is modeled as a differentiable Bernoulli random variable, and the loss is defined as the mutual information between the sampled subgraph and the original graph. By maximizing this objective, the framework learns edge importance scores and identifies informative structures. Based on these importance scores, we adopt an augmented Lagrangian approach with convergence guarantees to gradually impose sparsity during optimization, rather than removing edges in a one-shot manner. Moreover, GRAPHSPA integrates flatness-aware training into the sparsification process to optimize the encoder in a way that reduces sensitivity to residual noise, thereby ensuring robust generalization even without labels.

4.1 PROBLEM FORMULATION

Self-Supervised Objective. We adopt a self-supervised strategy to preserve the essential information of the original graph G. Specifically, we maximize the mutual information between the original graph G and the sparsified graph G_s by adopting the InfoNCE loss (van den Oord et al., 2018).

Let node embeddings be $\mathbf{H} = f_\theta(X, A_s)$ obtained from a GNN encoder parameterized by θ, where h_v denotes the embedding of node $v \in \mathcal{V}$. The pair (G, G_s) is treated as a positive sample, while negative samples $\tilde{G}_s$ are generated by randomly dropping a portion of edges from G. The contrastive loss is then defined as

$$\mathcal{L} = -\sum_{v \in \mathcal{V}} \log \frac{\exp(\mathrm{sim}(h_v^G, h_v^{G_s})/\beta)}{\sum_{u \in \mathcal{V}} \exp(\mathrm{sim}(h_v^G, h_u^{G_s})/\beta)}, \tag{6}$$

where $\mathrm{sim}(\cdot, \cdot)$ is a similarity function such as cosine similarity and β is a temperature parameter. This loss encourages the embeddings from G_s to remain consistent with those from G, ensuring that sparsification retains informative edges without using labels.

Edge Importance Learning via Bernoulli Subgraph Sampling. At each training iteration, we need to construct a sparsified subgraph to learn importance of individual egdes. A naive approach would be to randomly sample edges from the original graph, which incurs an exponential search space of $2^{|\mathcal{E}|}$ possible subgraphs and does not allow gradient propagation since edge selection is a discrete 0-1 decision. To address this, we relax the binary mask into a continuous probability through a learnable logit x_{ij}, which reflects the latent importance of edge (i, j). Through the Gumbel-Softmax relaxation (Jang et al., 2017), we obtain a continuous importance score $s_{ij} \in (0, 1)$:

$$s_{ij} = \sigma\left(\frac{\log \xi_{ij} - \log(1 - \xi_{ij}) + x_{ij}}{\tau}\right), \quad \xi_{ij} \sim \mathcal{U}(0, 1), \tag{7}$$

where $\sigma(\cdot)$ is the sigmoid function and $\tau > 0$ is a temperature parameter. We initialize $x_{ij} = 0$ so that all edges start with equal importance.

The importance score s_{ij} serves a dual role. It provides a differentiable relaxation of binary edge selection, and it determines the probability that edge (i, j) is selected when constructing a subgraph. Formally, each edge is sampled according to a Bernoulli distribution with selection probability s_{ij}:

$$A_s(i, j) \sim \text{Bernoulli}(s_{ij}), \quad \forall (i, j) \in \mathcal{E}. \tag{8}$$

In other words, edge (i, j) is included in the sampled subgraph with probability s_{ij} and excluded otherwise. By interpreting s_{ij} as both a trainable relaxation and a sampling probability, the model can generate subgraphs in a stochastic manner. This sampling mechanism enables exploration of diverse structural variants, ensuring that even edges with low scores are occasionally selected. As perfectly identifying and removing noisy edges is infeasible, this strategy prevents the model from prematurely discarding potentially informative connections while still encouraging sparsification.

In practice, we start from a high temperature τ to encourage exploration of diverse subgraphs and gradually decrease it following a cosine scheduling strategy. This allows the model to explore structural variants more freely in the early stage of training, while focusing on more deterministic edge selection in the later stage. Details of the ablation study on the temperature scheduling strategy are provided in Appendix D.3.

Flatness-Aware Training. To enhance robustness against residual noise and improve generalization performance, we adopt a flatness-aware training strategy based on a min–max optimization. Specifically, the sparsified subgraph G_s is sampled from the original graph G according to the importance score s_{ij}. We then optimize the following objective:

$$\min_{\theta} \max_{\|\epsilon\|_p \leq \rho} \mathcal{L}(G_s, \theta + \epsilon), \tag{9}$$

where θ denotes the encoder parameters, ϵ is a perturbation vector, and ρ is the perturbation radius. The inner maximization corresponds to injecting perturbations into the encoder parameters, which simulates worst-case deviations during training and mimics the corrupted message passing caused by noisy edges. The outer minimization then drives the model to learn representations that remain stable under such perturbations, thereby improving generalization performance and reducing sensitivity to residual noise. In other words, the encoder is guided toward flat minima that generalize well under residual noise conditions.

4.2 Constrained Optimization

To mitigate the irreversible information loss caused by one-shot criterion-based sparsification, our key idea is to gradually impose substantial sparsity onto the edges while maximally preserving information during training. However, the restriction on the number of edges is inherently non-differentiable due to the discrete nature of the ℓ_0 constraint, which makes direct optimization infeasible. A standard approach for such constrained problems is to employ Lagrangian duality or projected gradient descent. Yet, the discrete nature of the ℓ_0-norm makes Lagrangian duality infeasible, while projected gradient descent, despite its efficiency, often struggles with highly non-convex objectives in neural network optimization.

To balance the smooth optimization of Lagrangian methods with the efficiency of projection, we adopt an augmented Lagrangian relaxation inspired by ADMM (Boyd et al., 2011b). To impose sparsity, we introduce an auxiliary variable z with the equality constraint $x = z$, where z periodically stores the projected sparse solution. This leads to the following problem, where the sparsity constraint $\|z\|_0 \leq r|E|$ ensures that only $r \times |E|$ edges are retained:

$$\min_{x,z} \max_{\|\epsilon\|_p \leq \rho} \mathcal{L}(G_s, \theta + \epsilon) + I_{\|z\|_0 \leq r|E|}(z), \quad \text{s.t. } x = z, \tag{10}$$

where $I_{\|z\|_0 \leq r|E|}(z)$ is the indicator function of the sparsity constraint:

$$I_{\|z\|_0 \leq r|E|}(z) := \begin{cases} 0, & \|z\|_0 \leq r|E|, \\ \infty, & \text{otherwise.} \end{cases} \tag{11}$$

Algorithm 1 GraphSpa

Require: Target edge ratio r, total iterations T, dual-update interval K, penalty parameter λ, perturbation radius ρ, temperature τ

Initialize $x^{(0)}$
$u = 0$
for $t = 0$ in $T - 1$ **do**
  for each edge $(i, j) \in E$ **do**
    $\xi_{ij} \sim \mathcal{U}(0, 1)$
    $s_{ij}^{(t)} \leftarrow \sigma\left(\dfrac{\log \xi_{ij} - \log(1 - \xi_{ij}) + x_{ij}^{(t)}}{\tau}\right)$
    $A_s^{(t)}(i, j) \sim \text{Bernoulli}(s_{ij}^{(t)})$
  end for
  Construct subgraph $G_s^{(t)} = (V, A_s^{(t)})$
  if $t \bmod K = 0$ **then**
    $z^{(t+1)} \leftarrow \text{Proj}_{\|z\|_0 \le r|E|}\left(x^{(t)} + u^{(t)}\right)$
    $u^{(t+1)} \leftarrow u^{(t)} + x^{(t)} - z^{(t+1)}$
  else
    $z^{(t+1)} \leftarrow z^{(t)}, \quad u^{(t+1)} \leftarrow u^{(t)}$
  end if
  $x^{(t+1)} \leftarrow x^{(t)} - \eta^{(t)}\Big(\nabla_x \mathcal{L}(G_s^{(t)}, \theta^{(t)}) + \lambda(x^{(t)} - z^{(t)} + u^{(t)})\Big)$
  $\hat{\epsilon} \leftarrow \rho \cdot \dfrac{\nabla_\theta \mathcal{L}(G_s^{(t)}, \theta^{(t)})}{\|\nabla_\theta \mathcal{L}(G_s^{(t)}, \theta^{(t)})\|_2}$
  $\theta^{(t+1)} \leftarrow \theta^{(t)} - \eta^{(t)} \nabla_\theta \mathcal{L}(G_s^{(t)}, \theta^{(t)} + \hat{\epsilon})$
end for
return $\text{Proj}_{\|z\|_0 \le r|E|}(x^{(T)})$

To enforce $x = z$ during optimization, we introduce a scaled dual variable u and add a quadratic penalty term $\frac{\lambda}{2}\|x - z\|_2^2$, yielding the augmented Lagrangian relaxation:

$$\max_{u} \min_{x,z} \Big(\mathcal{L}(x, z, u) := \max_{\|\epsilon\|_p \le \rho} \mathcal{L}(G_s, \theta + \epsilon) + I_{\|z\|_0 \le r|E|}(z) - \tfrac{\lambda}{2}\|u\|_2^2 + \tfrac{\lambda}{2}\|x - z + u\|_2^2\Big). \quad (12)$$

Applying alternating minimization with respect to x and z, and dual ascent on u, we obtain the following optimization subproblems:

$$\begin{aligned} x_{k+1}, z_{k+1} &= \arg\min_{x,z} \max_{\|\epsilon\|_p \le \rho} \Big(\mathcal{L}(G_s, \theta + \epsilon) + I_{\|z\|_0 \le r|E|}(z) + \tfrac{\lambda}{2}\|x - z + u_k\|_2^2\Big), \\ u_{k+1} &= \arg\max_{u} \ \tfrac{\lambda}{2}\|x_{k+1} - z_{k+1} + u\|_2^2 - \tfrac{\lambda}{2}\|u\|_2^2. \end{aligned} \quad (13)$$

The z-update corresponds to a projection due to the indicator function, and the u-update reduces to a simple dual ascent step. Therefore, the iterative scheme becomes:

$$\begin{aligned} x_{k+1} &= \arg\min_{x} \max_{\|\epsilon\|_p \le \rho} \Big(\mathcal{L}(G_s, \theta + \epsilon) + \tfrac{\lambda}{2}\|x - z_k + u_k\|_2^2\Big), \\ z_{k+1} &= \text{Proj}_{\|z\|_0 \le r|E|}(x_{k+1} + u_k), \\ u_{k+1} &= u_k + x_{k+1} - z_{k+1}. \end{aligned} \quad (14)$$

Since the x-minimization cannot be solved in closed form, we approximate it by a single gradient descent step on the objective. This yields the practical update rules:

$$\begin{aligned} x_{k+1} &= x_k - \eta\Big(\nabla_x \mathcal{L}(G_s, \theta_k) + \lambda(x_k - z_k + u_k)\Big), \\ z_{k+1} &= \text{Proj}_{\|z\|_0 \le r|E|}(x_{k+1} + u_k), \\ u_{k+1} &= u_k + x_{k+1} - z_{k+1}. \end{aligned} \quad (15)$$

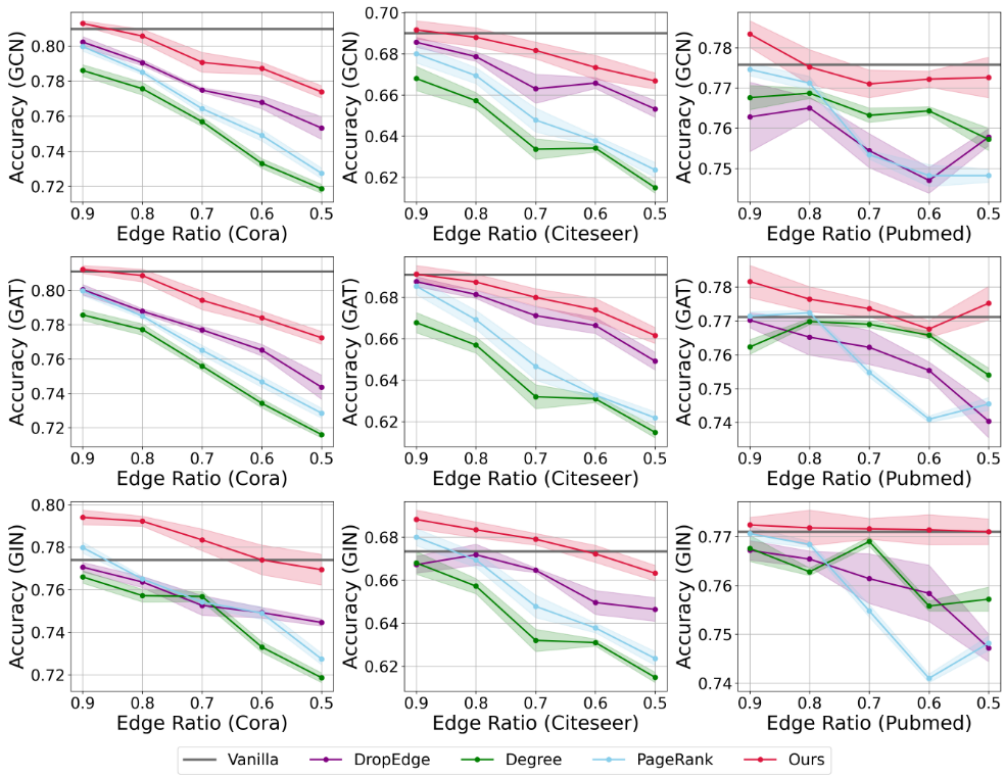

Figure 1: Node classification accuracy under different graph sparsity ratio on GCN/GAT/GIN across the Cora/Citeseer/Pubmed datasets. Results are reported as mean ± std over 5 random seeds.

During training, this procedure gradually aligns x with z, allowing continuous optimization between projection steps, and avoids the irreversible information loss of one-shot sparsification. In this way, the framework achieves progressive sparsification that preserves essential structural information under a hard ℓ_0 constraint, while benefiting from the stability of augmented Lagrangian optimization.

4.3 Noise-Resilient Encoder Optimization

While updating (x, z, u) with the augmented Lagrangian scheme, we simultaneously update the model parameters θ using the same loss function $\mathcal{L}$ applied to the sparsified subgraph G_s. By injecting perturbations into the GNN parameters, the encoder is trained in a flatness-aware manner, which reduces its sensitivity to residual noisy edges. As a result, the learned representations become more robust and generalizable, achieving improved performance even under conditions where residual noise persists in the graph. The perturbation vector is approximated as:

$$\hat{\epsilon} = \rho \frac{\nabla_\theta \mathcal{L}(G_s, \theta_k)}{\|\nabla_\theta \mathcal{L}(G_s, \theta_k)\|_2}, \tag{16}$$

and the parameter update is given by

$$\theta_{k+1} = \theta_k - \eta \nabla_\theta \mathcal{L}(G_s, \theta_k + \hat{\epsilon}). \tag{17}$$

Intuition. Each iteration of GraphSpa proceeds as follows: (i) a subgraph G_s is sampled using the current edge probabilities from x, with a high initial temperature gradually annealed via cosine scheduling to balance exploration and exploitation, (ii) the auxiliary variables z and u are updated every K steps to enforce the hard ℓ_0 constraint through projection and dual ascent, (iii) the edge logits x are updated while staying close to the sparsity-projected proxy z and simultaneously maximizing mutual information with the original graph to preserve informative structures, and (iv) the model parameters θ are optimized toward flatter minima via perturbation-based updates, reducing

sensitivity to residual noisy edges and mitigating overfitting. The overall procedure of our framework is summarized in Algorithm 1. We provide a theoretical guarantee that the x-minimization converges during training. The detailed proof of convergence is deferred to Appendix A.

5 EXPERIMENTS

In this section, we present experiments to validate the effectiveness of the proposed framework. We first introduce the experimental settings, then compare our method with several baselines that do not use labels, and finally provide analysis to highlight its advantages in terms of performance, generalization, and applicability under noisy graph settings.

5.1 EXPERIMENTAL SETUP

Datasets & Models. We evaluate our framework on three transductive benchmark datasets Cora, Citeseer, and Pubmed (Kipf & Welling, 2016). We adopt the public splits for all datasets, and dataset statistics are summarized in Appendix B. For backbone models, we use Graph Convolutional Network (GCN) (Kipf & Welling, 2016), Graph Attention Network (GAT) (Veličković et al., 2018), and Graph Isomorphism Network (GIN) (Xu et al., 2019).

Baselines. We compare our proposed method against the following sparsification strategies (i) Vanilla use original graph for training (ii) DropEdge (Rong et al., 2020) (iii) degree-based (Batagelj & Zaversnik, 2003) (iv) PageRank (Page et al., 1999). DropEdge reduces edge density uniformly, while degree-based and PageRank heuristically remove edges associated with nodes of low degree or low PageRank scores. PageRank method measures the relative importance of nodes in a graph by simulating random walks and thus prioritizes preserving edges linked to structurally important nodes. Further implementation details are provided in Appendix B.1.

5.2 PERFORMANCE ANALYSIS

Figure 1 reports the node classification accuracy under different edge retention ratios r, where r denotes the proportion of edges retained after sparsification. All results are reported as averages over 5 random seeds. At moderate sparsification levels such as $r = 0.9$, our method not only mitigates the adverse impact of edge removal but also consistently outperforms the vanilla backbone models across all three datasets. This suggests that removing redundant or noisy edges through sparsification enables the backbone to learn cleaner and more informative representations. When the retention ratio decreases to $r = 0.5$, both Cora and Citeseer show a natural performance drop. This is expected because graphs with relatively fewer edges are more likely to lose critical structural information once a large proportion of edges are removed. Nevertheless, our method still exhibits a much slower decline compared to DropEdge, degree-based, or PageRank-based heuristics, maintaining higher accuracy under aggressive sparsification. In contrast, on the Pubmed dataset, which contains substantially more edges, our method still achieves comparable performance to the vanilla backbone even at $r = 0.5$. This indicates that our sparsification strategy can effectively preserve the important structural information of the original graph. Overall, our method achieves the best performance across all edge retention ratios and datasets, demonstrating that it can effectively remove noisy or redundant edges while preserving essential structural information, even without any label supervision. The superior results on Pubmed further highlight that the benefits of our method scale with graph size, underscoring its practical applicability to large-scale real-world graphs.

5.3 ROBUSTNESS TO NOISY EDGES

If noisy edges remain after the sparsification process, they can distort node representations and significantly degrade the generalization performance of GNNs (Zügner et al., 2018). Previous studies have shown that existing sparsification methods fail to consistently remove all harmful connections (Chen et al., 2021). Therefore, it is necessary to make the model less sensitive to the remaining noisy edges. To evaluate the robustness of our method against such noise, we first sparsify the original graph by retaining $r = 0.5$ of the edges and then inject random edges following the protocol of Jin et al. (2021) to construct corrupted graphs. The source and destination nodes of injected edges are randomly sampled, and the noise ratio $r_{noise} \in \{0.1, 0.2, 0.3, 0.4, 0.5\}$ denotes the proportion of

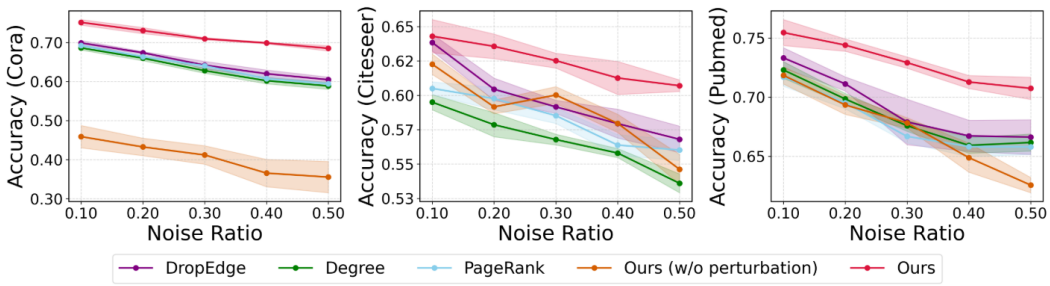

Figure 2: Node classification accuracy of GCNs under injected noisy edges after 50% edge sparsification with different noisy edge ratios. Results are reported as mean ± std over 5 random seeds.

injected edges relative to the number of edges after sparsification. We use a GCN model and report classification accuracy averaged over 5 runs on three benchmark datasets.

Figure 2 shows that as the noise ratio increases, the performance of existing methods deteriorates rapidly, revealing that GNN is vulnerable to remaining noisy edges. In particular, our method maintains higher accuracy by training the encoder in a flatness-aware manner during sparsification, which makes it less sensitive to noisy edges and improves generalization. An interesting observation is made on the Cora dataset. When sparsification was performed without flatness-aware training denoted as ours (w/o perturbation), the model exhibited poor performance, even worse than the baselines. This suggests that Cora, being a relatively small dataset, is more vulnerable to mis-trained encoders. Once the encoder is poorly optimized during sparsification, the erroneous representations are carried over into the downstream training stage, leading to severe performance degradation. In small graphs, even a few noisy or mis-specified edges can dominate the structural information, while insufficient training signals make it difficult to correct such errors. These findings highlight the necessity of flatness-aware training during sparsification to ensure noise-robust representations.

5.4 Qualitative Analysis

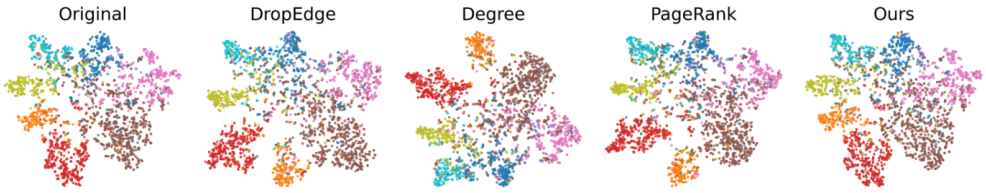

Figure 3: t-SNE visualization of node embeddings on the Pubmed after 50% edge sparsification.

Figure 3 presents the 2D t-SNE projections of node embeddings after removing 50% of the edges using different methods. As observed, the embeddings from our method exhibit a clustering structure consistent with the original graph, whereas other baselines show altered cluster distributions. This indirectly demonstrates that our sparsification strategy can more effectively preserve the structural information of the original graph. Moreover, our method produces compact yet informative subgraphs, enabling reliable graph learning without labels even under noisy conditions.

6 Conclusion

In this work, we proposed GraphSpa, a self-supervised graph sparsification framework that unifies constrained optimization with flatness-aware training. By modeling edges as differentiable Bernoulli variables and maximizing mutual information, GraphSpa learns informative structures without labels. Augmented Lagrangian scheme progressively enforces sparsity with convergence guarantees, while flatness-aware optimization mitigates residual noise. Experiments show that GraphSpa achieves strong accuracy across sparsity ratios, preserves structural integrity, and remains robust to noisy edges, establishing it as a principled approach for scalable and reliable graph learning.

ACKNOWLEDGMENT

Use unnumbered third level headings for the acknowledgments. All acknowledgments, including those to funding agencies, go at the end of the paper.

REFERENCES

Christina Baek, J Zico Kolter, and Aditi Raghunathan. Why is sam robust to label noise? In *International Conference on Learning Representations (ICLR)*, 2024.

Vladimir Batagelj and Matjaž Zaversnik. An $o(m)$ algorithm for cores decomposition of networks. *arXiv preprint arXiv:cs/0310049*, 2003.

Joshua Batson, Daniel A Spielman, Nikhil Srivastava, and Shang-Hua Teng. Spectral sparsification of graphs: Theory and algorithms. *Communications of the ACM*, 56(8):87–94, 2013.

Stephen Boyd, Neal Parikh, Eric Chu, Borja Peleato, and Jonathan Eckstein. *Distributed Optimization and Statistical Learning via the Alternating Direction Method of Multipliers*. Foundations and Trends in Machine Learning, 2011a.

Stephen Boyd, Neal Parikh, Eric Chu, Borja Peleato, and Jonathan Eckstein. Distributed optimization and statistical learning via the alternating direction method of multipliers. *Foundations and Trends in Machine Learning*, 3(1):1–122, 2011b. doi: 10.1561/2200000016.

Dongkwan Chen, Kyungwoo Shin, Tianxiang Zhang, Sung Ju Hwang, Kijung Shin, and Sung Ju Lee. Unified graph structured learning with randomly pruned message passing. In *Advances in Neural Information Processing Systems (NeurIPS)*, 2021.

Mingze Dong and Yuval Kluger. Towards understanding and reducing graph structural noise for gnns. In *Proceedings of the 2023 International Conference on Machine Learning (ICML)*, 2023.

Matthias Fey and Jan E. Lenssen. Pytorch geometric: Deep learning on irregularly structured input data. In *Proceedings of the International Conference on Learning Representations (ICLR) Workshop on Representation Learning on Graphs and Manifolds*, 2019.

Pierre Foret, Ariel Kleiner, Hossein Mobahi, and Behnam Neyshabur. Sharpness-aware minimization for efficiently improving generalization. In *International Conference on Learning Representations (ICLR)*, 2021.

Michelle Girvan and M. E. J. Newman. Community structure in social and biological networks. *Proceedings of the National Academy of Sciences*, 99(12):7821–7826, 2002.

Jing Guo, Yujie Wang, Ming Chen, Yu Zhang, and Xindong Wu. Unsupervised social event detection via hybrid graph contrastive learning and reinforced incremental clustering. *Knowledge-Based Systems*, 287:110289, 2024.

Weihua Hu, Matthias Fey, Marinka Zitnik, Yuxiao Dong, Hao Ren, Bowen Liu, Michela Catasta, and Jure Leskovec. Open graph benchmark: Datasets for machine learning on graphs. In *Advances in Neural Information Processing Systems (NeurIPS)*, 2020.

Eric Jang, Shixiang Gu, and Ben Poole. Categorical reparameterization with gumbel–softmax. In *International Conference on Learning Representations*, 2017. arXiv:1611.01144.

Wei Jin, Yao Ma, Xiaorui Liu, and Jiliang Tang. Node injection attacks on graphs via reinforcement learning. In *Proceedings of the 27th ACM SIGKDD International Conference on Knowledge Discovery & Data Mining (KDD)*, pp. 1398–1408, 2021.

Pham Duy Khanh, Hoang-Chau Luong, Boris S. Mordukhovich, and Dat Ba Tran. Fundamental convergence analysis of sharpness-aware minimization. In *Advances in Neural Information Processing Systems (NeurIPS)*, 2024. URL https://arxiv.org/abs/2401.08060.

Thomas N Kipf and Max Welling. Semi-supervised classification with graph convolutional networks. *arXiv preprint arXiv:1609.02907*, 2016.

Jintang Li, Ruofan Wu, Wangbin Sun, Liang Chen, Sheng Tian, Liang Zhu, Changhua Meng, Zibin Zheng, and Weiqiang Wang. MaskGAE: Masked graph modeling meets graph autoencoders. *CoRR*, abs/2205.10053, 2022.

Qimai Li, Xiao-Ming Wu, Hongwei Liu, Xiaotong Zhang, and Zhen Guan. Label efficient semi-supervised learning via graph filtering. *IEEE Transactions on Pattern Analysis and Machine Intelligence*, 2019. doi: 10.1109/TPAMI.2019.2960335.

Zhixun Li, Xin Sun, Yifan Luo, Yanqiao Zhu, Dingshuo Chen, Yingtao Luo, Xiangxin Zhou, Qiang Liu, Shu Wu, Liang Wang, et al. GSLB: The graph structure learning benchmark. In *Advances in Neural Information Processing Systems (NeurIPS)*, volume 36, 2024.

Yixin Liu, Shirui Pan, Ming Jin, Chuan Zhou, Feng Xia, and Philip S. Yu. Graph self-supervised learning: A survey. *CoRR*, abs/2103.00111, 2021.

Fan Luo, Wei Cheng, Wenchao Yu, Bo Zong, Haifeng Chen, Wei Zhang, and Haifeng Wang. Learning to Drop: Robust Graph Neural Network via Topological Denoising. In *Proceedings of the 38th International Conference on Machine Learning (ICML)*, 2021.

Lawrence Page, Sergey Brin, Rajeev Motwani, and Terry Winograd. The pagerank citation ranking: Bringing order to the web. Technical Report 1999-66, Stanford InfoLab, 1999. Previous number = SIDL-WP-1999-0120.

Adam Paszke, Sam Gross, Francisco Massa, Adam Lerer, James Bradbury, Gregory Chanan, Trevor Killeen, Zeming Lin, Natalia Gimelshein, Luca Antiga, Alban Desmaison, Andreas Kopf, Edward Yang, Zachary DeVito, Martin Raison, Alykhan Tejani, Sasank Chilamkurthy, Benoit Steiner, Lu Fang, Junjie Bai, and Soumith Chintala. Pytorch: An imperative style, high-performance deep learning library. In H. Wallach, H. Larochelle, A. Beygelzimer, F. d'Alché Buc, E. Fox, and R. Garnett (eds.), *Advances in Neural Information Processing Systems (NeurIPS 2019)*, volume 32, pp. 8024–8035, 2019.

Jiezhong Qiu and et al. Network embedding as matrix factorization: Unifying deepwalk, line, pte, and node2vec. In *WSDM*, 2018.

Yu Rong, Yatao Huang, Wenbing Xu, and Junzhou Huang. DropEdge: Towards deep graph convolutional networks on node classification. In *International Conference on Learning Representations (ICLR)*, 2020.

Venu Satuluri and Srinivasan Parthasarathy. Local graph sparsification. In *Proceedings of the 2011 ACM SIGMOD International Conference on Management of Data*, pp. 721–732. ACM, 2011.

Stanislav Sobolevsky and Alexander Belyi. Graph neural network inspired algorithm for unsupervised network community detection through modularity optimization. *Applied Network Science*, 7(1):1–15, 2022.

Aaron van den Oord, Yazhe Li, and Oriol Vinyals. Representation learning with contrastive predictive coding. In *Advances in Neural Information Processing Systems*. Curran Associates, Inc., 2018.

Petar Veličković, Guillem Cucurull, Arantxa Casanova, Adriana Romero, Pietro Liò, and Yoshua Bengio. Graph attention networks. In *Proceedings of the International Conference on Learning Representations (ICLR)*, 2018.

Petar Velickovic, William Fedus, William L Hamilton, Pietro Liò, Yoshua Bengio, and R. Devon Hjelm. Deep graph infomax. In *International Conference on Learning Representations (ICLR)*, 2019. Poster.

Xiaoyun Wang, Minhao Cheng, Joe Eaton, Cho-Jui Hsieh, and Felix Wu. Attack graph convolutional networks by adding fake nodes. In *arXiv preprint arXiv:1810.10751*, 2018.

Lirong Wu, Dongkun Luo, Keyulu Xu, Yuanchun Zhuang, et al. SUBLIME: A self-supervised learning framework for graphs via virtual node information maximization. In *International Conference on Machine Learning (ICML)*, 2023.

Dongkuan Xu, Wei Cheng, Dongsheng Luo, Haifeng Chen, and Xiang Zhang. InfoGCL: Information-aware graph contrastive learning. In *Advances in Neural Information Processing Systems (NeurIPS)*, pp. 30414–30425, 2021.

Keyulu Xu, Weihua Hu, Jure Leskovec, and Stefanie Jegelka. How powerful are graph neural networks? In *International Conference on Learning Representations (ICLR)*, 2019.

Zhilin Yang, William W. Cohen, and Ruslan Salakhutdinov. Revisiting semi-supervised learning with graph embeddings. In *International Conference on Machine Learning (ICML)*, pp. 40–48, 2016.

Rex Ying, Ruining He, Kaifeng Chen, Pong Eksombatchai, William L Hamilton, and Jure Leskovec. Graph convolutional neural networks for web-scale recommender systems. In *Proceedings of the 24th ACM SIGKDD International Conference on Knowledge Discovery & Data Mining*, pp. 974–983. ACM, 2018.

Jiaqi Zeng and Pengtao Xie. Contrastive self-supervised learning for graph classification. In *Proceedings of the AAAI Conference on Artificial Intelligence*, pp. 10824–10832. AAAI Press, 2021.

Muhan Zhang and Yixin Chen. Link prediction based on graph neural networks. In *Advances in Neural Information Processing Systems*, volume 31, 2018.

Xiaoxin Zheng et al. Graph Learning with Personalized PageRank for Semi-Supervised Node Classification. In *Proceedings of the 34th AAAI Conference on Artificial Intelligence (AAAI)*, 2020.

Jie Zhou, Ganqu Cui, Zhengyan Zhang, Cheng Yang, Zhiyuan Liu, Lifeng Wang, Changcheng Li, and Maosong Sun. Graph neural networks: A review of methods and applications. *arXiv preprint arXiv:1812.08434*, 2018.

Daniel Zügner, Amir Akbarnejad, and Stephan Günnemann. Adversarial attacks on neural networks for graph data. In *Proceedings of the 24th ACM SIGKDD International Conference on Knowledge Discovery & Data Mining (KDD)*, pp. 2847–2856, 2018.

SUPPLEMENTARY MATERIALS

A CONVERGENCE ANALYSIS

n this section, we establish the convergence of our flatness-aware sparsification framework. Our proof builds on the augmented Lagrangian method (Boyd et al., 2011a) and extends the fundamental convergence analysis of sharpness-aware minimization (Khanh et al., 2024), thereby providing theoretical guarantees for the stability of our approach.

A.1 ASSUMPTIONS

Assumption A.1. (Smoothness and Weak Convexity) The loss $\mathcal{L}(G_s^{(t)}, \theta)$ is β-smooth and μ-weakly convex in x.

Assumption A.2. (Lipschitz Gradient) The gradient of $\mathcal{L}$ with respect to x is Lipschitz, and stochastic gradients (if any) are unbiased and have bounded variance.

Assumption A.3. (Step Size) The step size $\{\eta^{(t)}\}$ is diminishing, satisfying

$$\sum_{t=1}^{\infty} \eta^{(t)} = \infty, \qquad \sum_{t=1}^{\infty} (\eta^{(t)})^2 < \infty.$$

Assumption A.4. (Perturbation Radius) The perturbation radius $\{\rho^{(t)}\}$ applies only to θ-updates and is bounded and/or diminishing, satisfying

$$\limsup_{t\to\infty} \rho^{(t)} < \tfrac{1}{\beta}, \qquad \sum_{t=1}^{\infty} \eta^{(t)} \rho^{(t)} < \infty.$$

Assumption A.5. (Strong Convexity of the Augmented Term) The penalty parameter satisfies $\lambda > \mu$, ensuring a strong convexity component in the augmented Lagrangian.

A.2 SMOOTHNESS AND CONVEXITY OF THE AUGMENTED LAGRANGIAN

Lemma A.1. Under Assumptions A.1–A.5, the augmented Lagrangian

$$\hat{\mathcal{L}}(x, z, u, \theta) = \mathcal{L}(G_s^{(t)}, \theta) + I_{\|z\|_0 \le r|E|}(z) - \tfrac{\lambda}{2}\|u\|^2 + \tfrac{\lambda}{2}\|x - z + u\|^2$$

is $(\beta + \lambda)$-smooth and $(\lambda - \mu)$-strongly convex in x.

Proof. From β-smoothness of $\mathcal{L}$ and quadratic penalty $\frac{\lambda}{2}\|x-z+u\|^2$, we obtain $(\beta+\lambda)$-smoothness. Since $\lambda > \mu$, the strong convexity term dominates the μ-weak convexity, yielding $(\lambda - \mu)$-strong convexity.

A.3 CONVERGENCE OF x-MINIMIZATION

The x-update is given by

$$x^{(t+1)} = x^{(t)} - \eta^{(t)} \Big(\nabla_x \mathcal{L}(G_s^{(t)}, \theta) + \lambda (x^{(t)} - z^{(t)} + u^{(t)}) \Big).$$

Define

$$g^{(t)} := \nabla_x \mathcal{L}(G_s^{(t)}, \theta) + \lambda (x^{(t)} - z^{(t)} + u^{(t)}).$$

By β-smoothness of $\hat{\mathcal{L}}$, we have

$$\hat{\mathcal{L}}(x^{(t+1)}) \le \hat{\mathcal{L}}(x^{(t)}) - \eta^{(t)} \langle \nabla \hat{\mathcal{L}}(x^{(t)}), g^{(t)} \rangle + \tfrac{\beta (\eta^{(t)})^2}{2} \|g^{(t)}\|^2. \tag{18}$$

Lemma A.2. (Projection Consistency) The projection step $z^{(t)} = \Pi_{\mathcal{C}}(x^{(t)} + u^{(t)})$ ensures feasibility of the sparsity constraint $\|z\|_0 \le r|E|$ and preserves boundedness of $\{z^{(t)}\}$.

Proof. By non-expansiveness of Euclidean projection,

$$\|z^{(t+1)} - z^{(t)}\| \le \|(x^{(t+1)} - x^{(t)}) + (u^{(t+1)} - u^{(t)})\|.$$

A.4 Convergence of θ Updates

The θ-update uses SAM perturbations:

$$\hat{\epsilon}^{(t)} = \rho^{(t)} \frac{\nabla_\theta \mathcal{L}(G_s^{(t)}, \theta^{(t)})}{\|\nabla_\theta \mathcal{L}(G_s^{(t)}, \theta^{(t)})\|}, \qquad \theta^{(t+1)} = \theta^{(t)} - \eta^{(t)} \nabla_\theta \mathcal{L}(G_s^{(t)}, \theta^{(t)} + \hat{\epsilon}^{(t)}).$$

Lemma A.3. (Lemma B.1 of (Khanh et al., 2024)) Let $\{a^{(t)}\}, \{b^{(t)}\}, \{c^{(t)}\}$ be nonnegative sequences satisfying

$$a^{(t+1)} - a^{(t)} \leq b^{(t)} a^{(t)} + c^{(t)},$$

with conditions

$$\sum_{t=1}^{\infty} b^{(t)} = \infty, \qquad \sum_{t=1}^{\infty} c^{(t)} < \infty, \qquad \sum_{t=1}^{\infty} b^{(t)} a^{(t)} < \infty.$$

Then $a^{(t)} \to 0$ as $t \to \infty$.

Lemma A.4. (Perturbation Stability) Under Assumptions A.2–A.4, the perturbed gradient satisfies

$$\|\nabla_\theta \mathcal{L}(G_s^{(t)}, \theta^{(t)} + \hat{\epsilon}^{(t)}) - \nabla_\theta \mathcal{L}(G_s^{(t)}, \theta^{(t)})\| \leq \beta \rho^{(t)}.$$

Proof. By β-smoothness of $\mathcal{L}$, the deviation due to $\hat{\epsilon}^{(t)}$ is upper bounded by $\beta \|\hat{\epsilon}^{(t)}\| = \beta \rho^{(t)}$.

A.5 Convergence to Stationary Points

Theorem A.1. (Stationarity of Limit Points) Under Assumptions A.1–A.5, the iterates of Algorithm 1 satisfy

$$\nabla_x \hat{\mathcal{L}}(x^{(t)}, z^{(t)}, u^{(t)}, \theta^{(t)}) \to 0, \qquad \nabla_\theta \mathcal{L}(G_s^{(t)}, \theta^{(t)}) \to 0, \quad \text{as } t \to \infty.$$

Thus, every limit point $(\bar{x}, \bar{z}, \bar{u}, \bar{\theta})$ is a stationary point of the augmented Lagrangian with SAM-regularized parameter updates.

Proof. From equation 18, we see that $\hat{\mathcal{L}}(x^{(t)})$ decreases up to error terms proportional to $(\eta^{(t)})^2$. By Assumptions A.3–A.4, $\sum_t \eta^{(t)} \rho^{(t)} < \infty$, ensuring bounded cumulative perturbation. For θ, Lemma A.4 guarantees perturbation errors vanish as $\rho^{(t)} \to 0$. Applying Lemma A.3 (Robbins–Siegmund type argument), we obtain

$$\lim_{t \to \infty} \|\nabla_x \hat{\mathcal{L}}(x^{(t)})\| = 0, \qquad \lim_{t \to \infty} \|\nabla_\theta \mathcal{L}(G_s^{(t)}, \theta^{(t)})\| = 0.$$

Therefore, every accumulation point is stationary in both (x, z, u) and θ.

A.6 Corollaries

Corollary A.1. (Expected Convergence) If the gradient is estimated via unbiased stochastic samples with bounded variance, then the expected squared gradient norm satisfies

$$\mathbb{E}\big[\|\nabla \hat{\mathcal{L}}(x^{(t)})\|^2\big] \to 0 \quad \text{as } t \to \infty.$$

Proof. This follows directly from Theorem A.1 and the assumption that stochastic gradients are unbiased with bounded variance (Hypothesis A.2). Applying Lemma A.3, we obtain the convergence of expected gradient norms.

Corollary A.2. (Convergence Rate) If the step size is chosen as $\eta^{(t)} = \frac{1}{\sqrt{t}}$ and the perturbation radius satisfies $\rho^{(t)} = O(\frac{1}{\sqrt{t}})$, then

$$\min_{1 \leq t \leq T} \mathbb{E}\big[\|\nabla \hat{\mathcal{L}}(x^{(t)})\|^2\big] = O\Big(\tfrac{1}{\sqrt{T}}\Big).$$

Proof. The rate follows by combining the descent inequality equation 18, bounded perturbation from Lemma A.4, and the standard analysis of diminishing step sizes.

Scaling with Graph Size. An important implication of our analysis is how sparsification interacts with graph size. Suppose the graph has N nodes with average degree $\bar{d}$, so that $|E| \approx N\bar{d}$. For a fixed sparsification ratio ρ, the number of preserved edges is $r|E|$. As $N \to \infty$, the redundancy of edges increases, and the variance introduced by random edge removal vanishes:

$$\frac{\mathrm{Var}[\text{edge sampling}]}{|E|} \to 0.$$

This provides an intuitive explanation of why our sharpness-aware sparsification benefits become more pronounced on large-scale graphs such as Pubmed.

B Experimental Settings

Dataset	#Nodes	#Edges	#Features	#Classes	Split ratio
Cora	2,708	5,429	1,433	7	120/500/1000
Citeseer	3,327	4,732	3,703	6	140/500/1000
PubMed	19,717	44,338	500	3	60/500/1000

Table 1: Statistics of benchmark datasets.

Table 1 summarizes the datasets used in our experiments, including the number of nodes, edges, features, classes and split ratios. We adopt the public splits from (Yang et al., 2016).

B.1 Implementation Details

Hyper-parameter	**Value / Search Space**
Epochs	200
Learning rate (η)	0.001
Learning rate schedule	cosine
Weight decay	0.005
Dropout	0.5
Hidden units	128
Attention heads	8
β	0.2
τ (Gumbel temperature)	cosine schedule
Perturbation radius (ρ)	{0.01, 0.05, 0.1, 0.2, 0.5, 0.8, 1.0}
Dual-update interval (K)	{1, 2, 5, 10, 20, 40}
Penalty parameter (λ)	{0.0001, 0.001, 0.01, 0.1}

Table 2: Hyperparameter details used for GraphSpa

All experiments are implemented in PyTorch (Paszke et al., 2019) and PyTorch Geometric (Fey & Lenssen, 2019), and conducted on a single NVIDIA RTX 2080 Ti (11GB) GPU. Each experiment is repeated with 5 different random seeds, and we report the average accuracy together with the standard deviation. We adopt GCN, GAT, and GIN as backbone in our experiments. For GCN, we use a two-layer architecture with 128 hidden units, weight decay of 0.005, and dropout rate of 0.5. GAT also has two layers with 128 hidden units, and employs 8 attention heads and a dropout rate of 0.5. For GIN, we use a two-layer network with 128 hidden units and dropout rate of 0.5. We adopt a cosine learning rate schedule across all models. In our method, several hyperparameters play a critical role, including the perturbation radius (ρ), dual-update interval (K), and penalty parameter (λ). These hyperparameters are tuned via grid search for each dataset, and the final results are reported using the best configuration selected from the search space summarized in Table 2.

C Computation Complexity Analysis

C.1 Sparsification Complexity

The computational complexity of our self-supervised sparsification framework can be decomposed into three main components: (i) sparsification, (ii) contrastive loss computation, and (iii) encoder training.

Sparsification stage. Each epoch involves parameterizing edge scores $x \in \mathbb{R}^{|E|}$, applying the Gumbel–Sigmoid relaxation, and constructing the normalized sparse adjacency, which requires

$$O(|E|).$$

In addition, every K iterations a projection step is performed at a cost of

$$O(|E| \log |E|),$$

which amortizes to $\frac{1}{K} O(|E| \log |E|)$ per epoch.

Contrastive loss Computation. Constructing the similarity matrix between embeddings $z_1, z_2 \in \mathbb{R}^{N \times d}$ has a complexity of

$$O(N^2 d).$$

When negative sampling or mini-batch contrastive learning is adopted, this reduces to

$$O(Nd).$$

Encoder training. For each forward/backward pass, the GNN encoder requires

$$O(|E|d).$$

Since SAM optimization performs two such passes per epoch, the encoder cost is effectively doubled, though it remains $O(|E|d)$ in asymptotic order.

Total complexity. Putting everything together, the per-epoch complexity is

$$O(|E|d + N^2 d) + \tfrac{1}{K} O(|E| \log |E|),$$

and for T epochs, the total complexity becomes

$$O\big(T \cdot (|E|d + N^2 d) + \tfrac{T}{K} |E| \log |E|\big).$$

Simplification. The number of edges can be approximated by the average degree $\bar{d}_{avg}$ as $|E| \approx \frac{1}{2} N \bar{d}_{avg}$. Thus, the edge-related term simplifies to $|E|d \approx N \bar{d}_{avg} d$. For sparse graphs where $\bar{d}_{avg} = O(1)$, we obtain $|E|d = O(Nd)$, showing that the edge cost grows linearly with N and d.

Final complexity. After simplification, the dominant cost depends on the loss calculation scheme:

- **Full contrastive learning:** all node pairs are compared, so the $N^2 d$ term dominates, leading to
$$\boxed{O(T \cdot (N^2 d + Nd))}.$$
- **Negative sampling:** only sampled edges are considered, so message passing dominates, giving
$$\boxed{O(T \cdot |E|d)} \quad \text{which simplifies to } O(TNd) \text{ for sparse graphs.}$$

C.2 Sparsification Complexity Comparision

Compared with heuristic sparsification methods such as DropEdge, degree-based, and centrality-based sparsification, our method has a higher asymptotic complexity due to the additional contrastive loss and SAM-based optimization. However, in practice both the number of epochs T and embedding dimension d are typically small constants (e.g., $T \leq 200$, $d \leq 128$). As a result, the practical runtime of GraphSpa is comparable to these baselines, while achieving better accuracy and robustness.

Method	Time Complexity	Explanation
DropEdge	$O(\|E\|)$	Random edge sampling per epoch: $O(\|E\|)$
Degree	$O(\|E\| \log \|E\|)$	Degree computation: $O(\|E\|)$ + Edge sorting: $O(\|E\| \log \|E\|)$
PageRank	$O(N\|E\|)$	Betweenness centrality via Brandes: $O(N\|E\|)$
GraphSpa	$O(TN^2d)$ or $O(T\|E\|d)$	Subgraph sampling: $O(\|E\|)$ Contrastive loss computation: $O(N^2d)$ or $O(\|E\|d)$ Encoder training: $O(Nd)$

Table 3: Time complexity analysis for baseline sparsification methods and GRAPHSPA.

D ABLATION STUDIES

D.1 IMPACT OF FLATNESS-AWARE TRAINING DURING SPARSIFICATION

Method	Edge ratio 0.9	0.8	0.7	0.6	0.5
GraphSpa (Frozen)	76.60 ± 0.21	76.06 ± 2.80	76.46 ± 1.11	75.16 ± 1.80	74.44 ± 1.24
GraphSpa (Adam)	76.52 ± 1.49	75.90 ± 2.52	76.66 ± 1.28	75.58 ± 1.46	74.86 ± 1.02
GraphSpa	**78.34** ± **0.76**	**77.52** ± **1.04**	**77.10** ± **0.74**	**76.72** ± **0.45**	**77.26** ± **1.13**

Table 4: Ablation study on encoder training during sparsification on Pubmed. Results are reported as mean ± std over 5 random seeds.

Table 4 presents the ablation results on the Pubmed dataset, comparing three settings: Frozen Encoder, Adam, and SAM. The results highlight that encoder training during sparsification is crucial for achieving good generalization and robustness to noisy edges. Freezing the encoder significantly degrades accuracy since the embeddings cannot adapt to the evolving sparse graph structure. Training with Adam provides moderate results but is less robust across edge ratios. In contrast, SAM consistently achieves the best performance, demonstrating that flatness-aware optimization enhances stability during training and yields more reliable performance under varying sparsity levels.

D.2 SENSITIVITY TO HYPERPARAMETER ρ

The perturbation radius ρ introduced by SAM is a critical hyperparameter that controls the extent of parameter perturbations during optimization. Choosing an appropriate ρ is essential for balancing robustness and training stability.

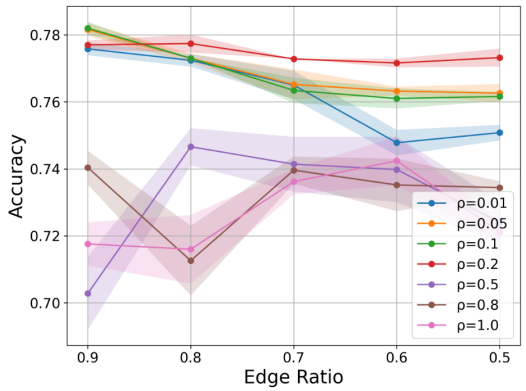

Figure 4: Sensitivity of performance to the SAM perturbation radius ρ on Pubmed. Results are reported as mean ± std over 5 random seeds.

- **Large ρ:** When ρ is large, the optimizer explores flatter regions in the loss landscape, which can potentially improve generalization and robustness. However, overly large perturbations may destabilize training or hinder convergence, leading to degraded performance.
- **Small ρ:** When ρ is too small, it may result in limited robustness gains, as the perturbations are not sufficient to promote significant flatness in the parameter space.

We conducted experiments by varying $\rho \in \{0.01, 0.05, 0.1, 0.2, 0.5, 0.8, 1.0\}$ to evaluate its impact on performance. Figure 4 illustrates the test accuracy across different edge ratios. Small ρ (e.g., 0.01) provides only minor improvements, while very large ρ (e.g., 0.5 or above) causes unstable training and significant degradation. An intermediate range (e.g., $\rho = 0.1$ or $\rho = 0.2$) yields the best trade-off between robustness and stability.

D.3 Effects of τ Scheduling

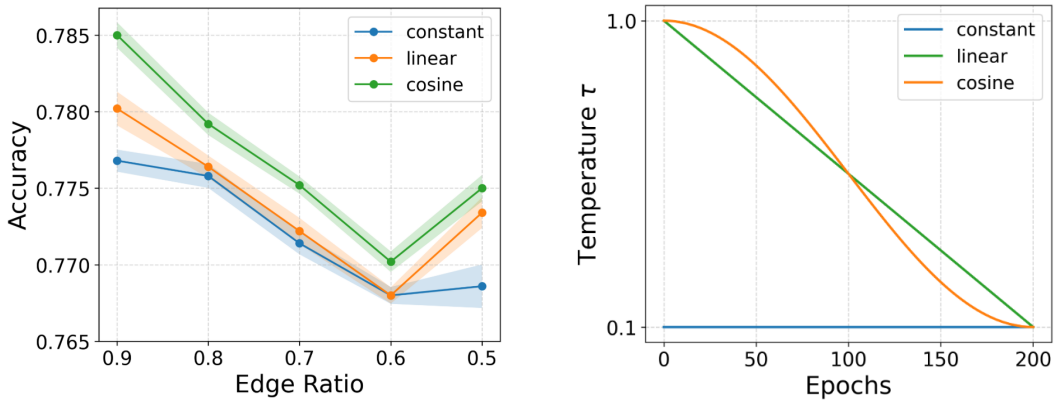

(a) Test Accuracy (b) Schedules

Figure 5: Effects of τ scheduling. (a) Sparsification accuracy across different sparsification ratios for constant τ compared with linear and cosine schedules. (b) Illustration of τ scheduling strategies, where the cosine schedule maintains a higher τ in the early phase and decreases later for exploitation.

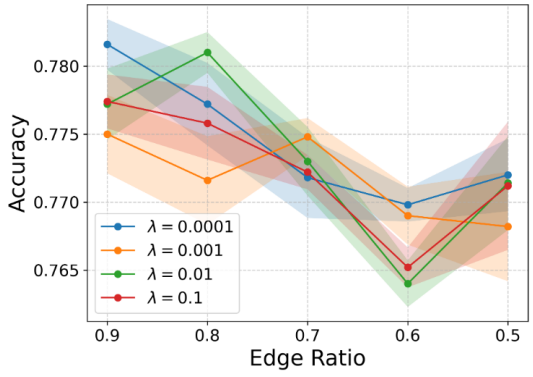

Figure 6: Effect of different penalty parameters λ on validation accuracy on Pubmed under varying edge ratios. Results are reported as mean ± std over 5 random seeds.

In addition to fixed τ, we investigate different scheduling strategies to dynamically adjust the temperature during training. As shown in Figure 5, we compare sparsification performance under different τ settings. (a) demonstrates the effect of constant τ versus linear and cosine scheduling on sparsification accuracy across various sparsification ratios. (b) illustrates the scheduling dynamics of τ, where the cosine schedule starts with a relatively higher τ to encourage exploration of diverse subgraphs through broader edge distributions, and then gradually decays to enhance exploitation in the

later phase. This gradual transition from exploration to exploitation explains why cosine scheduling consistently achieves better performance compared to both constant and linear schedules.

D.4 Effects of Penalty Parameter λ

We investigate the effect of different choices of the penalty parameter λ on accuracy across various edge ratios. Figure 6 reports the average accuracy with standard deviation for $\lambda \in \{10^{-4}, 10^{-3}, 10^{-2}, 10^{-1}\}$ under edge ratios ranging from 0.9 to 0.5. We observe that larger values of λ such as 10^{-1} generally alleviate the accuracy drop at moderate edge ratios but degrade the performance when the sparsification becomes more aggressive. In contrast, smaller values such as $\lambda = 10^{-4}$ yield competitive performance at higher edge ratios but fail to stabilize under heavier sparsification. This highlights the trade-off between enforcing the sparsity constraint more strongly via larger λ and preserving model accuracy under different sparsity levels. In particular, while $\lambda = 10^{-2}$ achieves the highest performance around edge ratio 0.8, its accuracy decreases significantly at 0.6, indicating that the choice of λ must be carefully balanced depending on the target sparsity.